Environmental Science & Technology

pubs.acs.org/est

Article

Influence of Physical Perturbation on Fe(II) Supply in Coastal Marine Sediments

Ulf Lueder, Markus Maisch, Katja Laufer, Bo Barker Jørgensen, Andreas Kappler, and Caroline Schmidt*

Cite This: *Environ. Sci. Technol.* 2020, 54, 3209−3218

Read Online

ACCESS | Metrics & More | Article Recommendations | Supporting Information

ABSTRACT: Iron (Fe) biogeochemistry in marine sediments is driven by redox transformations creating Fe(II) and Fe(III) gradients. As sediments are physically mixed by wave action or bioturbation, Fe gradients re-establish regularly. In order to identify the response of dissolved Fe(II) (Fe^{2+}) and Fe mineral phases toward mixing processes, we performed voltammetric microsensor measurements, sequential Fe extractions, and Mössbauer spectroscopy of 12 h light−dark cycle incubated marine coastal sediment. Fe^{2+} decreased during 7 days of undisturbed incubation from approximately 400 to 60 μM. In the first 2−4 days of incubation, Fe^{2+} accumulated up to 100 μM in the top 2 mm due to Fe(III) photoreduction. After physical perturbation at day 7, Fe^{2+} was remobilized reaching concentrations of 320 μM in 30 mm depth, which decreased to below detection limit within 2 days afterward. Mössbauer spectroscopy showed that the relative abundance of metastable iron-sulfur mineral phases (FeS_x) increased during initial incubation and decreased together with pyrite (FeS_2) after perturbation. We show that Fe^{2+} mobilization in marine sediments is stimulated by chemical changes caused by physical disturbances impacting the Fe redox distribution. Our study suggests that, in addition to microbial and abiotic Fe(III) reduction, including Fe(III) photoreduction, physical mixing processes induce chemical changes providing sediments and the inhabiting microbial community with Fe^{2+}.

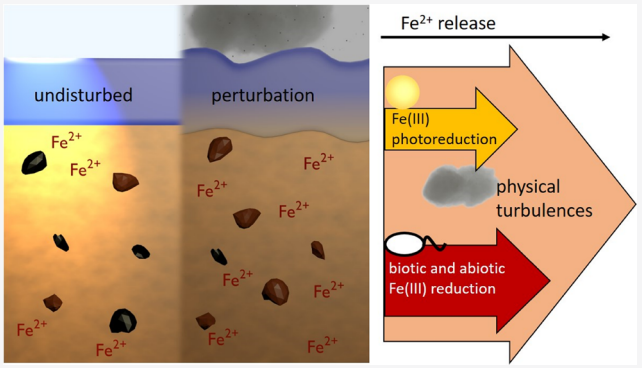

Downloaded via UNIV TUEBINGEN on March 17, 2020 at 15:33:45 (UTC).
See https://pubs.acs.org/sharingguidelines for options on how to legitimately share published articles.

INTRODUCTION

Iron (Fe) is an important redox-active element in coastal marine sediments. It is an essential element for many living organisms and can be used as a substrate, that is, as an electron donor, energy source, or electron acceptor, for growth by Fe-metabolizing bacteria.[1] In the environment, Fe is cycled between its two main redox states, ferrous (Fe(II)) and ferric iron (Fe(III)), by many biotic and abiotic reactions.[2] Microbial Fe(II) oxidation can be catalyzed by microaerophilic, nitrate-reducing, or anoxygenic phototrophic microorganisms, which are ubiquitously present in coastal marine sediments.[3−6] Fe(II) can also be abiotically oxidized by oxygen (O_2), reactive nitrogen species, or manganese(IV) minerals.[2] Additionally, Fe(II) can abiotically be produced in sunlit sediments by Fe(III) photoreduction.[7] In anoxic sediments, Fe(III) is reduced to Fe(II) by heterotrophic or autotrophic Fe(III)-reducing microorganisms coupled to the oxidation of organic compounds or hydrogen[8−10] or by abiotic Fe(III) reduction by redox-active natural organic matter or dissolved sulfide (H_2S + HS^- + S^{2-}).[11−13] Upward diffusion of dissolved Fe(II) (Fe^{2+}) along prevailing redox gradients and re-oxidation by, for example, O_2,[14] as well as mineral precipitation or dissolution lead to decreasing Fe^{2+} concentrations in the sedimentary pore water toward the sediment−water interface.[15−17]

Fe redox changes have important consequences for the biogeochemical cycling of other elements, for example, via precipitation of mineral phases such as iron (oxyhydr)oxides, carbonates, phosphates, or sulfides[15,18,19] or sorption of heavy metals or nutrients to Fe minerals.[20−23] Fe(III) (oxyhydr)-oxides that are able to rapidly react with sulfide ("reactive iron"[12,24−26]) control the distribution of dissolved sulfide in the pore water, which is produced by bacterial sulfate reduction in marine sediments.[24,27,28] During the reaction of Fe(III) (oxyhydr)oxides with sulfide, Fe^{2+} is formed, which further reacts with sulfide to form various iron-sulfide minerals.[12] The resulting Fe-S phases precipitate as metastable Fe(II) monosulfide (FeS) or as pyrite (FeS_2), which is the most stable form of Fe sulfides under environmental conditions.[11,12,29−31] Those formed minerals as well as dissolved and particulate Fe species are mainly transported by sedimentation and diffusion processes in stagnant coastal

Received: October 18, 2019
Revised: February 5, 2020
Accepted: February 15, 2020
Published: February 15, 2020

ACS Publications © 2020 American Chemical Society

https://dx.doi.org/10.1021/acs.est.9b06278
Environ. Sci. Technol. 2020, 54, 3209−3218

sediments without physical perturbation.[15] In contrast, in bioturbated or wave-influenced sediments, advection is an important transport process, and iron- or FeS-containing minerals can be actively transported toward the sediment surface or be buried deeper into the sediment where they undergo oxidation or reduction accomplishing rapid recycling processes.[18,32,33] In shallow bays and estuaries, interactions between currents and waves lead to extensive sediment resuspension and transport,[34] with wind-induced wave motion reaching the seabed down to 12 m water depth in some estuaries.[35−37] More extensive disturbances of the sediment, for example, caused by a storm or rigorous tidal movement, can completely rearrange the sediment layers. This leads to shifts in sediment pore water geochemical gradients. O_2 profiles establish rapidly in sediments and respond quickly to temperature and light intensity changes.[38,39] However, it is not known how fast Fe^{2+} profiles react upon changing geochemical conditions, especially considering the occurrence of sulfur compounds in marine sediments with complex interactions between Fe^{2+}, Fe colloids, Fe(III) (oxyhydr)oxides, and sulfide and the formation of highly reactive metastable Fe-S phases. The availability and speciation of Fe strongly influences the biogeochemistry in sediments not only by serving as a nutrient or substrate for growth for microorganisms but also by changing the availability of other elements by precipitation reactions or sorption. As the upper millimeters of marine sediments are frequently mixed by wave action or tidal movement, it is important to identify the impact of physical perturbation on sediments and concomitant changes in Fe^{2+} gradients.

Here, we quantified Fe^{2+} concentrations and determined mineralogical changes of solid-phase iron during incubation of marine sediment and after a simulated storm event. The objectives of this study were (i) to understand the consequences of heavy perturbations caused during a storm event on the Fe^{2+} concentration gradient and Fe redox stability in the sediment and (ii) to decipher mechanisms for fluctuations of sedimentary Fe^{2+} gradients.

MATERIALS AND METHODS

Sediment Core Incubations and Experimental Approach. Marine bulk sediment (from 0.5 m depth) and seawater were collected from a brackish shallow estuary, Norsminde Fjord, Denmark[3] (March 2017), near its narrow entrance to the Baltic Sea and kept in the dark in containers at 4 °C until further processing. In the lab, stones and macrofauna were removed from the sediment in order to enable microsensor application, and 5 cm of homogenized sediment were filled into cut 50 mL syringes, overlaid with 4 cm Norsminde Fjord water (artificial sediment cores). Homogenization of the sampled sediment was done to ensure homogeneous and reproducible starting conditions of the experiment. The artificial sediment cores were continuously aerated and refilled with oxic Norsminde Fjord water (salinity 18.8, pH 8.6) to compensate evaporation. The sediment cores were incubated in a 12 h light−dark cycle with a combination of two LED lamps (Samsung SI-P8V151DB1US, 14 W, 3000 K and SMD 2835, 15 W, 6000 K) and an adjusted light intensity of 250−300 μmol photons m^{-2} s^{-1} using a spherical light meter (ULM-500 and US-SQS/L sensor, Walz, Germany). In order to prevent light penetration from the sides, the cores were wrapped in aluminum foil from the sediment−water interface downward. After 7 days of incubation, the sediment cores were completely mixed using a spatula and consecutively bubbled with ambient air through a silicon tube with an attached needle using a fish tank pump. The bubbling lasted for 1 h and was strong enough to continuously mix the sediment and keep it in the suspension simulating a storm event. The cores were incubated for three more days before the sediment was again rigorously mixed and aerated for 1 h. Sediment cores that were prepared for incubation are shown in Figure S1.

In order to compare concentration changes of solid phase and dissolved Fe, 17 artificial sediment cores were prepared at the beginning of the experiment. Microsensor measurements of Fe^{2+} and O_2 were related to results obtained from sequential solid-phase Fe extractions and ^{57}Fe Mössbauer spectroscopy. Thirteen of the artificial sediment cores that were prepared at the beginning of the experiment were used to monitor the development of Fe^{2+} and O_2 gradients with microsensors. Each day, another sediment core was used (sacrificial setup). At days 0, 2, and 7 of undisturbed sediment core incubation and after the simulated storm event, samples for Mössbauer spectroscopy were taken from these artificial sediment cores after the microsensor measurements. For sequential Fe extractions, three artificial sediment cores were prepared, of which one replicate was used for extraction after 0 and 7 days of undisturbed incubation and directly after the simulated storm. In order to test how sensitive the Fe^{2+} release from the sediment is toward physical perturbation, we tested the impact of physical sediment movement and aeration on the Fe^{2+} mobilization. For that, another artificial sediment core was prepared, and cyclic voltammetric scans for Fe^{2+} detection were run in (i) the sediment core that was incubated for 7 days, (ii) a homogenized layer of the sediment after slicing the core, and (iii) the supernatant after centrifuging (oxic conditions, maximal disturbance) the homogenized sediment layer for 5 min at 12,045*g*. A detailed scheme of the experimental approach is shown in Figure S2.

The DOC concentration of the sediment pore water was quantified with a carbon analyzer (Multi N/C 2100 s, Analytik Jena, Germany).

Microsensor Measurements. Microsensor measurements were performed daily after 6 h of light exposure and approximately 30 min after the simulated storm event. Fe^{2+} concentration profiles were recorded by voltammetry using a DLK-70 web-potentiostat (Analytical Instrument Systems, Flemington, NJ) and a standard three-electrode system with a lab-constructed glass-encased 100 μm gold amalgam (Au/Hg) working electrode,[40] a solid-state Ag wire coated with a Ag/AgCl reference electrode, and a Pt wire counter electrode. Cyclic voltammograms were collected by scanning from −0.05 to −1.8 V and back with at a scan rate of 2000 mV s^{-1} and with an initial potential of −0.05 V held for 2 s for conditioning the electrode. Before each scan, a potential of −0.9 V was applied for 5 s to clean the electrode surface electrochemically. Calibration for Fe^{2+} was done by applying the pilot ion method with Mn^{2+}.[40,41] Ten scans were run at every measurement depth, and the last three voltammograms were analyzed using the VOLTINT program for Matlab.[42] Fe^{2+} concentrations were recorded 1 mm above and directly at the sediment surface and in 0.5, 1, 1.5, 2, 3, 4, 6, 10, 15, and 30 mm depth. Additionally, cyclic voltammetry was performed during a simulated storm event in approximately 30 mm depth.

Dissolved O_2 was measured with a 100 μm tip diameter Clark-type O_2 microelectrode (Unisense, Denmark) as

https://dx.doi.org/10.1021/acs.est.9b06278
Environ. Sci. Technol. 2020, 54, 3209−3218

described by Revsbech.[43] A two-point calibration was performed in fully air-saturated or anoxic Norsminde Fjord water. O_2 concentration profiles were recorded with the software Sensor Trace Suite (Unisense, Denmark) in triplicate with a spatial resolution of 200 μm. Error bars show the standard deviation of triplicate measurements. Light penetration depth was determined by measuring the scalar irradiance with lab-constructed light sensors[44] connected to a spectrometer (USB4000-XR1-ES, Ocean Optics, Germany) with the software SpectraSuite (Ocean Optics, Germany). High-resolution profiles of H_2S and pH were additionally measured using glass microelectrodes (Unisense, Denmark) at the end of the incubation period. O_2 and redox potential profiles were measured with glass microelectrodes (Unisense, Denmark) in in situ sediment cores in the field shortly before and 2 days after a strong storm event at the sampling field site in October 2013.

Sequential Fe Extractions. Sequential Fe extractions were used to follow changes in solid-phase Fe redox transformation over time. Anoxic Na-acetate (pH 5), 0.5 and 6 M HCl were used to consecutively dissolve different Fe phases with increasing crystallinity. Na-acetate was chosen for extracting adsorbed Fe(II)[45,46] and Fe in Fe sulfides,[47] 0.5 M HCl for extracting poorly crystalline, amorphous Fe (oxyhydr)oxides and (remaining) reduced Fe(II) species such as $FeCO_3$ or FeS,[48] and 6 M HCl for extracting the higher crystalline, remaining reactive Fe fractions of the sediment. Artificial sediment cores were sliced under anoxic conditions (100% N_2, remaining O_2 < 100 ppm) at 0−2, 2−4, 9−11, and 29−31 mm depth, and approximately 0.5 g of homogenized sediment of each sliced depth was added into Eppendorf tubes. Pore water was removed after centrifugation (5 min, 12,045g), and 1 mL of anoxic Na-acetate solution (pH 5) was added to the pellet, mixed, and incubated (dark, 24 h). After centrifugation (5 min, 12,045g), 100 μL of the supernatant was stabilized with 900 μL anoxic 1 M HCl, and the residual Na-acetate was discarded. One milliliter of anoxic 0.5 M HCl was added to the pellet, mixed, and incubated in the dark for 2 h. After centrifugation, stabilization of 100 μL of supernatant in 900 μL of anoxic 1 M HCl, and removal of the residual supernatant, 1 mL of anoxic 6 M HCl was added to the pellet, mixed and incubated for 24 h in the dark as the last extraction step. The extractants were subsequently analyzed in technical triplicate by the spectrophotometric Ferrozine assay.[49]

Fe Mineral Analysis. The sediment for ^{57}Fe Mössbauer spectroscopy was collected under anoxic conditions (100% N_2) from the sediment cores in a depth of approximately 30 mm at the beginning (day 0) and after 2 and 7 days of incubation, as well as shortly after the first simulated storm event. The sediment was loaded into a Plexiglass holder and was stored anoxically at −80 °C until measurement. Mössbauer spectroscopy was performed in transmission mode, and absorption spectra were collected at 77 and 5 K. Sample analysis was carried out using the Voigt Based Fitting (VBF) routine[50] with an α^{57}Fe foil (7 μm thick, room temperature) for center shift calibration. The sediment for X-ray diffraction (XRD) analysis was anoxically collected in a depth of approximately 30 mm after 7 days of incubation and analyzed twice as (i) native anoxic wet sediment and (ii) dried under oxic conditions. Detailed XRD parameters are shown in the Supporting Information.

RESULTS AND DISCUSSION

Development of Fe^{2+} Gradients during Undisturbed Incubation after Preparation of Artificial Sediment Cores. One hour after preparation of the artificial sediment cores from the homogenized marine sediment, highest Fe^{2+} concentrations of approximately 400 μM were measured in 30 mm depth with decreasing Fe^{2+} concentrations upward (Figure 1). Fe^{2+} concentrations continuously decreased over time in the undisturbed sediment cores throughout the complete depth gradient during the following 7 days of incubation to approximately 60 μM in 30 mm depth (Figure 1). This decrease in Fe^{2+} can be attributed to the fact that geochemical gradients first need to establish in the freshly prepared sediment cores, leading to a change of the sedimentary Fe speciation and the resulting gradients by Fe^{2+} adsorption to minerals, ongoing Fe redox reactions (e.g., Fe^{2+} oxidation), and consequent Fe phase transitions between the dissolved, adsorbed, and mineral fractions (including colloids). After the preparation of the artificial sediment cores, O_2 concentrations were quite low (50 μM in the water column, 1 mm penetration into the sediment; Figure 1), indicating high O_2 consuming processes and a reduced state of the sediment. However, oxygenic photosynthesis in the sediment led to O_2 supersaturation[51,52] within 2 days of undisturbed incubation (Figure 1 and Figure S3), thus enhancing abiotic Fe^{2+} oxidation in oxic sediment layers. In deeper and anoxic sediment layers, Fe^{2+} is produced by abiotic and biotic Fe(III) reduction, diffuses upward, and is oxidized by different processes, for example, by abiotic oxidation by O_2[14] or by microbial Fe^{2+} oxidation.[2] Therefore, increasing Fe^{2+} concentrations with depth can be expected.[15−17] Fe^{2+} concentrations

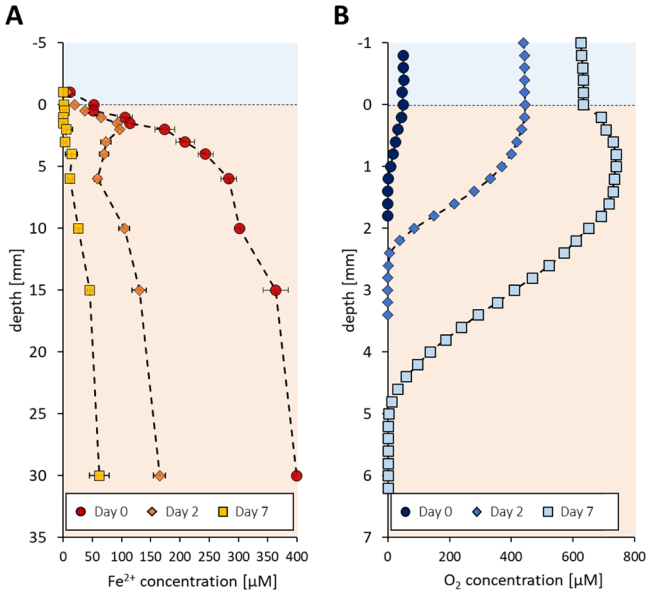

Figure 1. Concentration profiles after 6 h of light exposure in 12 h light−dark lab-incubated artificial marine sediment cores at the start (day 0) and after 2 and 7 days of undisturbed incubation. Note the different scales of the y axes. (A) Fe^{2+} concentration profiles. Error bars show standard deviation of triplicate voltammograms. (B) O_2 concentration profiles. O_2 concentrations were low at day 0 due to storage after sampling in airtight and dark containers. O_2 accumulation in the sediment during the experimental run is a combination of both, diffusion from the overlying water column and oxygenic sedimentary photosynthetic activity.

https://dx.doi.org/10.1021/acs.est.9b06278
Environ. Sci. Technol. 2020, 54, 3209−3218

of up to 100 μM in the top 2 mm of the sediment were quantified during the first 2−4 days of incubation (Figure 1). Fe^{2+} production in light-penetrated, oxic sediment layers has very recently been demonstrated to be caused by Fe(III) photoreduction.[7] The Fe^{2+} concentration measured in the top sediment layers after 2 days of undisturbed light−dark incubation was 60% of the concentration in 30 mm depth (approximately 170 μM), which is in the same range as previously observed in laboratory light-incubated freshwater sediments.[7] In the incubated marine sediment, light penetrates 2.2 mm (Figure S4). Besides the presence of light, there are some necessary geochemical prerequisites for Fe(III) photoreduction, such as the complexation of Fe(III) by organic carbon.[53] In fact, the sediment used for this study is characterized by high dissolved organic carbon concentrations in the pore water (84.5 ± 14.4 mg L^{-1}), which allows for the formation of such Fe(III)−organic complexes, as confirmed by voltammetry.[54]

Impact of Physical Perturbation on Fe^{2+} Gradients. Extensive physical mixing after 7 days of undisturbed sediment core incubation simulated a storm event and introduced O_2 into the sediment. This led to extensive re-mobilization and release of Fe^{2+} of up to 320 μM (in 30 mm depth) 30 min after the storm event (Figure 2). The simulation of the storm event

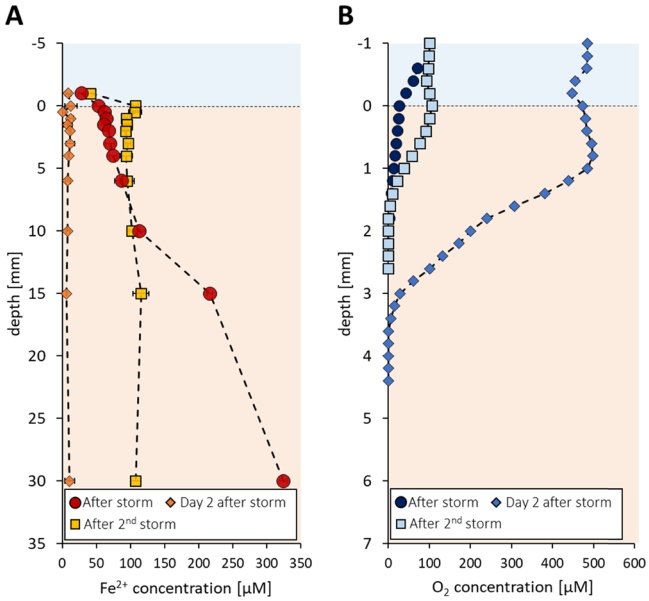

Figure 2. Concentration profiles measured in 12 h light−dark lab-incubated artificial marine sediment cores approximately 30 min after a simulated storm event (labeled "After storm"), after 2 days of undisturbed incubation after 6 h of light exposure ("Day 2 after storm"), and approximately 30 min after a second simulated storm event ("After 2nd storm"). Note the different scales of the *y* axes. (A) Fe^{2+} concentration profiles. Error bars show standard deviation of triplicate voltammograms. (B) O_2 concentration profiles.

was done after 7 days of undisturbed incubation as Fe^{2+} concentrations did not considerably change since 2 days assuming equilibrium of Fe^{2+} was established (Figure S5). Despite the aeration of the sediment for 1 h, the sediment pore water was clearly undersaturated with respect to O_2 (Figure 2). Reduced or mobilized sedimentary compounds that got in contact with O_2 during the simulated storm event or afterward during sediment settling removed large parts of the introduced O_2 via oxidation. The persistence of Fe^{2+} in the sediment pore water shortly after the storm event was potentially increased due to slower abiotic Fe^{2+} oxidation by O_2 at undersaturated O_2 conditions and generally slower abiotic Fe^{2+} oxidation kinetics by O_2 in seawater compared to freshwater due to higher salinity.[14] After physical perturbation the sediment re-fractionates by particle size during settling, which presumably leads to different geochemical conditions at different sediment depths. Larger and heavier minerals potentially settle faster than smaller minerals with higher surface area and consequently higher reactivity, which can presumably be found closer to the sediment−water interface. Therefore, pore space or the amount and size of Fe minerals might differ with sediment depth potentially influencing diffusion, dissolution, or sorption of Fe^{2+}. Voltammetric Fe^{2+} measurements performed during the simulated storm event showed the immediate release of Fe^{2+} (Figure S6). The Fe^{2+} profile after the storm represents the result of Fe^{2+} production (during the storm event) and consumption, including Fe^{2+} oxidation by O_2 in the top millimeters or microbial depletion processes. Due to the rate at which Fe^{2+} was mobilized (a few hundred μM within minutes), microbial Fe(III) reduction as sole source of Fe^{2+} is unlikely. For comparison, Laufer et al.[55] determined maximum Fe(III) reduction rates in the Norsminde Fjord sediment to be in the range of 180−590 μM day^{-1} suggesting that microbial Fe(III) reduction is too slow to account for the sole mechanism for all the observed Fe^{2+} mobilization during the simulated storm event. Possible other mechanisms for the observed Fe^{2+} release are discussed below considering results obtained by Mössbauer spectroscopy and sequential Fe solid-phase extractions. The mobilized Fe^{2+} decreased to below detection limit throughout the sediment column already within 2 days of subsequent undisturbed incubation (Figure 2). After additional 3 days of undisturbed light−dark incubation, simulation of a further storm event led to an immediate but lower re-mobilization of Fe^{2+} (~110 μM) into the pore water (Figure 2). This indicates that the incubated artificial sediment cores are depletive toward Fe^{2+} mobilization probably due to lacking renewability of the sedimentary system compared to in situ conditions. The mobilization of Fe^{2+} by the simulated storm event also led to micromolar concentrations (30−40 μM) in the water column (Figure 2), caused by the mixing of the water column with the sediment. The Fe^{2+} might be taken up by aquatic organisms before it gets oxidized, for example, by O_2. In marine waters, concentrations of dissolved Fe naturally are only in the pico- to nanomolar range.[56−58] Compared to other Fe(II) sources to the water column, such as diffusional Fe flux from sediments (micromolar range Fe m^{-2} d^{-1}),[59] aquatic Fe(III) photoreduction (production of nanomolar concentrations)[60,61] or Fe input from rivers, where Fe is primarily present in the form of ferric oxides,[62] the occasional Fe^{2+} input into the water column induced by storm events might therefore represent a significant Fe^{2+} source also to the marine water column.

The extreme sensitivity of Fe^{2+} mobilization from the sediments to physical disturbance and introduction of oxidants was demonstrated in a separate experiment. Fe^{2+} measurements with voltammetric microsensors were performed in a homogenized sediment core (incubated for 7 days without physical disturbance) and compared to measurements in homogenized slices of the sediment from three depths (0−2, 9−11, and 29−31 mm) and in the pore water of sliced, centrifuged sediment layers. While only 15 μM Fe^{2+} were

https://dx.doi.org/10.1021/acs.est.9b06278
Environ. Sci. Technol. 2020, 54, 3209−3218

measured in 10 mm depth in the intact sediment core, the Fe^{2+} concentration in the corresponding sliced and homogenized and therefore disturbed, sediment layer was 240 μM, that is, 16 times higher than Fe^{2+} concentrations in the undisturbed sediment cores (Figure S7). In 30 mm depth in the intact sediment core, Fe^{2+} (90 μM) was still about 2.5 times lower compared to the gently prepared homogenized sediment slice (230 μM) (Figure S7). These experiments highlight that physically disturbing processes are able to mobilize Fe^{2+} from the sediment, despite the simultaneous introduction of oxidants, and potentially increase its bioavailability as a nutrient or substrate for various microorganisms. Wave and tidal movement as well as bioturbation represent perturbation processes that constantly proceed in natural sediments, leading to particle shearing and sediment reworking.[63,64] In shallow coastal waters, bottom shear stress generated by tidal currents and wave movements is responsible for sediment resuspension into the water column, sediment mixing, and transport processes.[34,65] The critical shear stress needed for sediment movement may vary widely and depends on the type of the sediment and its degree of compaction.[36,66] Wind-induced waves have been observed to resuspend sediment in water depths up to 2−12 m in many estuaries.[36,37] Storms are even recognized to be the dominant physical force to suspend sediment on continental shelfs.[37] Based on our data, movement of the sediment would have a strong impact on the release of Fe^{2+} into the pore water and overlying seawater.

The in situ effects of storms to produce disturbed sediment and readjustment of geochemical gradients were also demonstrated by comparing O_2 and redox potential profiles of in situ measurements in sediment cores taken before and 2 days after a strong natural storm at the sampling field site (Supporting Information). Even 2 days after the storm, the redox potential measured in the sediment was still more positive even in a sediment depth of 14 mm compared to the redox potential measured before the storm (Figure S8), showing the relevance of storms for disturbing the sediment in the environment. The more positive redox potential in the upper 14 mm of the sediment measured after the storm (Figure S8) illustrates the more oxidized conditions of the sediment and that the geochemical gradients of the sediment are still in the process of readjusting to reach the same state as measured before the storm. The shape of the recorded O_2 concentration profiles (Figure S8) differed before and 2 days after the storm, indicating higher consumption of O_2 in the sediment after the storm. Due to mixing processes, reduced compounds can get oxidized, and fresh organic matter enters the sediment, leading to higher aerobic microbial respiration. Due to the time point of the storm (October 2013), low photosynthetic activity did not lead to O_2 supersaturation in the sediment. Besides heavy sediment perturbation caused by storms, already minor sediment mixing processes such as bioturbation affect the sediment geochemistry. Thamdrup et al.[33] pointed out the importance of bioturbation in sedimentary Fe cycling by transporting redox-active substrates across the oxic-anoxic interface, that is, Fe(III) to anoxic layers, where microbial and abiotic Fe(III) reduction occurs, and reversely, Fe(II) toward the oxic sediment surface where it gets oxidized by microbial and chemical reactions.[18]

Impact of Physical Perturbation on O_2 and Sulfide Geochemistry. Photosynthetic organisms are also mixed during physical perturbation. However, in comparison to Fe^{2+} gradients, the O_2 gradients re-establish faster in sediment cores[9,11,12] as oxygenic photosynthesis responds immediately to incoming light. Steady-state O_2 concentrations are reached rapidly, and O_2 concentrations change dynamically depending on changes in light intensity.[67,68] Oxygenic photosynthesis leads to supersaturation of O_2 in sediment pore water during illumination.[51,52,69] O_2 concentrations dramatically decreased in the sediment after the simulated storm event (Figure 2), presumably by reactions of O_2 with reduced sediment constituents. However, already 2 days after undisturbed light−dark incubation, O_2 supersaturation was reached in the incubated artificial sediment cores (Figure S3), whereas Fe^{2+} in the sediment pore water still was decreasing across the complete redox gradient, thereby influencing the whole sedimentary redox system. O_2 supersaturation of up to 600 μM re-established within a day after the simulated storm (Figure S3).

Apart from the influence by O_2, the Fe geochemistry in marine sediments is strongly influenced by sulfur species, which are involved in various chemical or microbially mediated redox reactions.[28] While Fe^{2+} is removed from the sediment pore water by precipitation as Fe sulfide minerals, it is released during their oxidation.[70] We did not detect dissolved sulfide by microsensor measurements in the incubated sediment cores shortly before or after the simulated storm event (data not shown). This lack of sulfide indicates that there is enough reactive iron present in this marine sediment to readily react with dissolved sulfide, potentially strongly controlling its pore water concentrations and (bio)availability.[12,24,25] Dissolved sulfide is likely produced constantly by bacterial sulfate reduction in the sediment[27] but is instantaneously removed by chemical reactions (e.g., by the formation of metastable FeS phases or even by reaction with FeS minerals to produce FeS_2[71]), leading to non-detectable (<1 μM) concentrations of dissolved sulfide in the pore water. In support of the formation of such Fe-S species, we recorded a voltammetric signal that resembles dissolved FeS clusters[72−74] directly after the initial preparation of the homogenized sediment cores throughout the entire core and in smaller amounts directly after the simulated storm event. Also, dissolved FeS clusters could be detected during the simulated storm event simultaneously to the detection of Fe^{2+}. Dissolved FeS clusters can form without immediate precipitation of solid FeS[75] but are indicative of solid amorphous FeS to be present in the sediment as well.[72] Dissolved FeS clusters were measurable only for a short time after the simulated storm and then disappeared within a day, highlighting the high reactivity of these species toward precipitation as FeS mineral phases and the importance of sulfur for the Fe redox system in the sediment. In marine sediments, FeS_2 usually is the most abundant Fe sulfide mineral,[76] and its rapid formation has been shown.[31,77] FeS_2 can be oxidized by O_2 or Fe^{3+} releasing Fe^{2+} is into the sedimentary pore water[78,79] according to eqs 1 and 2:

$$FeS_2 + 3.5O_2 + H_2O \rightarrow Fe^{2+} + 2SO_4^{2-} + 2H^+ \quad (1)$$

$$FeS_2 + 14Fe^{3+} + 8H_2O \rightarrow 15Fe^{2+} + 2SO_4^{2-} + 16H^+ \quad (2)$$

Physical perturbations transport FeS_2 to oxic sediment layers, where it is chemically oxidized by O_2[33,80] especially when the FeS_2 particles are small, leading to increased Fe^{2+} concentration in the sedimentary pore water. Additionally, O_2 that was introduced during the physical perturbation abiotically oxidizes Fe^{2+}, thereby forming Fe^{3+}, which in turn further

https://dx.doi.org/10.1021/acs.est.9b06278
Environ. Sci. Technol. 2020, 54, 3209−3218

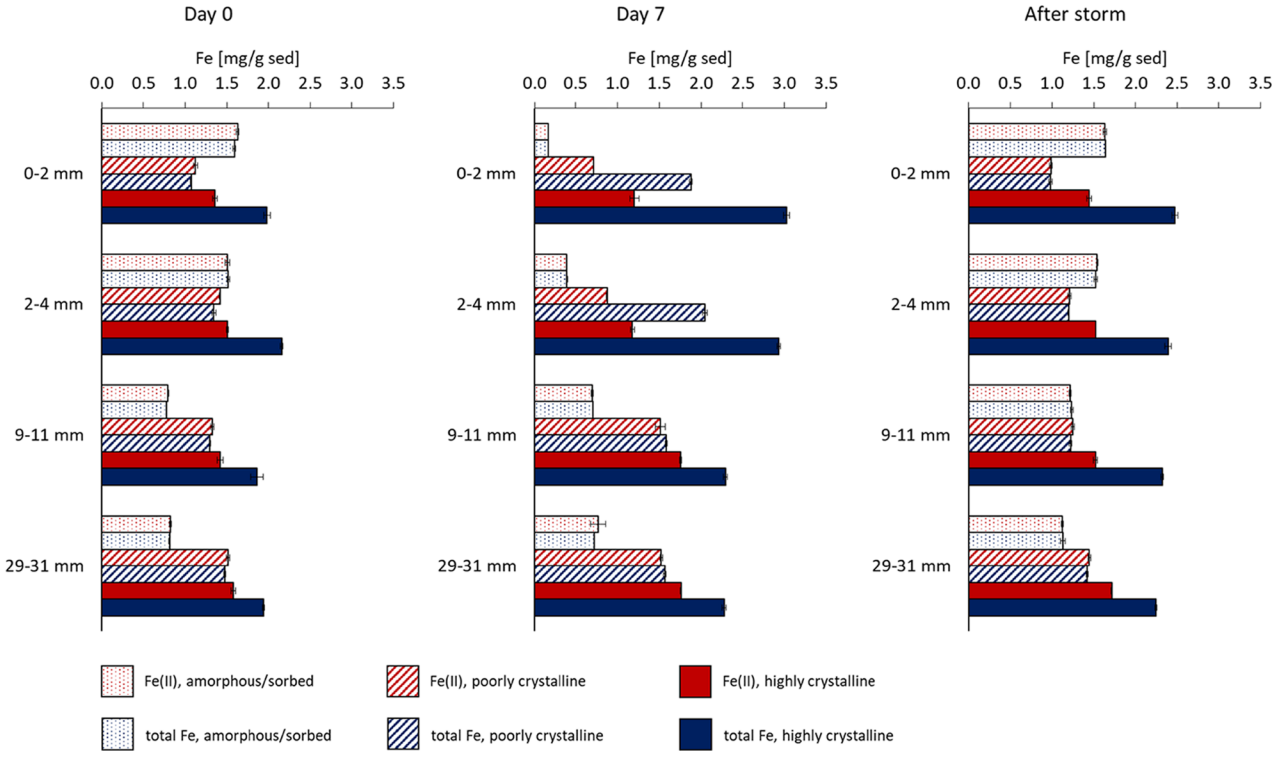

Figure 3. Sequential Fe extractions of different sliced sediment layers from sediment cores at the beginning (Day 0) and after 7 days (Day 7) of undisturbed incubation and shortly after a simulated storm event (After storm). Error bars show standard deviation of technical triplicate.

oxidizes FeS_2, leading to additional accumulation of Fe^{2+} in the pore water.

Fe Solid-Phase Crystallinity Changes. Sequential dissolution of different iron pools by different extractants allows insights into Fe crystallinity changes.[81] One hour after preparation of the artificial sediment cores, the adsorbed Fe fraction (on Fe(III) (oxyhydr)oxides and poorly crystalline carbonates) and Fe from FeS[47]; extracted by 1 M Na acetate, pH 5) and the poorly crystalline Fe mineral fraction (extracted by 0.5 M HCl) were all in the reduced state of Fe(II). Only the fraction of highest Fe crystallinity (extracted by 6 M HCl) contained Fe(III) (19−32%) (Figure 3). After 7 days of incubation, there was a shift from adsorbed/amorphous Fe phases (decrease from 1.17 mg Fe g^{-1} sediment averaged over depth; 25.49% of total Fe) after preparation of the sediment cores to 0.50 mg Fe g^{-1} sediment (10.12% of total Fe after 7 days of undisturbed incubation) toward higher crystalline Fe phases. There was an increase of poorly and highly crystalline Fe phases averaged over depth from 3.14 mg Fe g^{-1} sediment (74.51% of total Fe) to 4.40 mg Fe g^{-1} sediment (89.88% of total Fe) during incubation, with an increasing relative amount of Fe(III) observed (Figure 3), potentially caused by oxidation of adsorbed Fe(II) or Fe(II) minerals and mineral restructuring by Ostwald ripening processes.[82] This change in crystallinity during undisturbed incubation of the sediment was most pronounced in the top 4 mm. In contrast, after the simulated storm event, amorphous Fe mineral phases increased again to concentrations close to the initial state (1.38 mg Fe g^{-1} sediment averaged over depth) (Figure 3). The total amount of solid-phase Fe slightly increased during the 7 days of undisturbed incubation from 4.59 to 4.89 mg Fe g^{-1} sediment and to 4.94 mg Fe g^{-1} sediment averaged for all sediment depths after the simulated storm event. The data suggest that during undisturbed incubation, Fe mineralogy is mostly driven by an increase in crystallinity, potentially due to Ostwald ripening or continuous Fe(II)-catalyzed dissolution and re-precipitation. However, physical perturbation and concomitant sediment reworking seem to physically break larger mineral particles into smaller particles or at least break apart aggregates of minerals, with the consequence of a higher surface area and thus higher reactivity toward abiotic and biotic processes.[83,84] The smaller mineral particles presumably dissolve and re-precipitate as poorly crystalline Fe minerals, leading to regeneration of the sedimentary amorphous Fe phases. Settlement of the sediment after physical perturbation potentially leads to the formation of a sediment suspension for a certain time. This means that O_2 or other dissolved species of the pore water do not need to diffuse to Fe minerals but have an enhanced accessibility to the mineral surfaces, leading to more redox reactions or precipitation reactions compared to during undisturbed conditions. The formation of more amorphous Fe phases likely has consequences for the Fe bioavailability to microorganisms that use Fe(II) as a substrate or nutrient. The crystallinity of Fe minerals determines the rate and extent of microbial Fe(III) reduction.[85,86] By providing more less crystalline Fe phases to the sediment, microbially catalyzed Fe redox reactions are presumably enhanced. We suggest that constant mixing of the sediment, for example, by waves, prevents mineral ripening and increases the amount of dissolved or colloidal and more reactive Fe phases, thereby driving a dynamic and very reactive redox environment.

Transformation of Fe Mineral Phases after Physical Perturbation. The Fe mineralogy in the solid phase during incubation and after the storm event was identified by Mössbauer spectroscopy and XRD. Mössbauer spectra collected at 77 K showed similar properties for all measured samples collected from 30 mm depth at different time points (Figure S10). Additional measurements at 5 K revealed a

https://dx.doi.org/10.1021/acs.est.9b06278
Environ. Sci. Technol. 2020, 54, 3209−3218

poorly defined sextet in the recorded Mössbauer spectra (Figure S11), potentially resembling a metastable Fe-sulfur mineral phase that is present in the measured sediment samples of all time points (detailed Mössbauer spectroscopy data are shown in the Supporting Information (Figures S9 and S10 and Table S1). In accordance with Wan et al.[87] and Thiel et al.,[71] this phase was denoted as metastable FeS_x, representing a yet unknown Fe mineral phase undergoing magnetic ordering at 5 K. Besides the metastable FeS_x, non-magnetically ordered Fe(II) (oxyhydr)oxides and FeS_2 were detected as Fe(II) phases. Applying the VBF fit model to the 5 K spectra,[50] the relative abundances of the three iron phases varied slightly during incubation (Figure 4). An increase in the

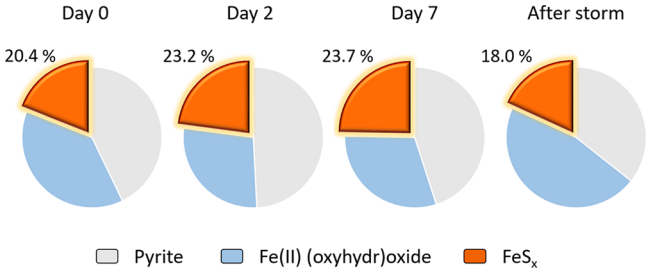

Figure 4. Relative abundances of pyrite, an Fe(II) mineral phase and metastable FeS_x mineral phases in the sediment cores in a depth of 30 mm over the course of undisturbed 12 h light−dark incubation (Days 0, 2, and 7) and shortly after a simulated storm event (After storm) determined by Mössbauer spectroscopy.

relative abundance of FeS_x from initial 20.4 ± 2.9 to 23.7 ± 1.9% after 7 days of undisturbed incubation and the decrease back to 18.0 ± 1.3% after the stimulated storm event suggest that, during undisturbed incubation, Fe^{2+} reacts rapidly with sulfide or another intermediate sulfur species to form metastable and highly reactive FeS_x phases.[11,87,88] Physical perturbation led to partial removal of FeS_x, for example, due to oxidation by O_2 entering the sediment during mixing or presumably as a result of breaking up amorphous FeS_x minerals by shearing forces, leading to smaller minerals with higher surface area and reactivity toward abiotic or biotic redox reactions and eventual dissolution of minerals. The accumulation of FeS_x during incubation and the subsequent partial removal after sediment perturbation deciphers one of the mechanisms responsible for the fluctuations of Fe^{2+} in the sediment pore water. Besides the metastable FeS_x, FeS_2 is present as another Fe sulfide mineral in the sediment cores and represents the quantitatively dominant Fe(II) phase (45 ± 0.3% after 7 days of incubation) before the simulated storm event. Its relative abundance dropped together with the FeS_x phases after the simulated storm event to 35.9 ± 0.6% (Figure 4), although FeS_2 is thermodynamically more stable than Fe monosulfides.[89] The presence of FeS_2 was confirmed by XRD. Detailed XRD results are shown in the Supporting Information and Figure S12. This decrease in the relative abundance of FeS_2 indicates that pyrite oxidation takes place in the sediment by either O_2 or Fe^{3+} forming Fe^{2+} during the physical perturbation. The fast decrease of Fe^{2+} after the simulated storm event (Figure 2) compared to Fe^{2+} concentrations measured during the mixing (Figure S6) shows that oxidation of FeS_2 and FeS_x is enhanced by the introduction of O_2 and the increased accessibility of the Fe sulfide mineral surfaces in the suspension during the mixing, which lead to elevated net concentrations of Fe^{2+} in the sediment pore water. During undisturbed incubation, oxidation of FeS_2 and FeS_x is slowed down or stopped due the lowered concentrations or the absence of O_2 and diminished accessibility of the mineral surfaces. Therefore, formation of Fe sulfide minerals, adsorption of Fe^{2+} and upward diffusion, and near-surface oxidation dominate during undisturbed conditions, leading to decreasing Fe^{2+} concentrations in the sediment pore water.

Environmental Implications. In the present study, we showed that physical perturbation induced, for example, by storms, bioturbation, or wave/tidal movement, is able to strongly impact the Fe geochemistry in marine sediments by changing the prevalent biogeochemical conditions, which shift the predominant Fe phases from highly crystalline Fe minerals into more poorly or amorphous Fe phases and partly oxidize metastable FeS_x or FeS_2, thereby potentially releasing Fe^{2+} into the pore water. So far, only abiotic and biotic Fe(III) reduction were considered to be sources of Fe^{2+} in marine sediments.[8,9,13,15,18] On the other hand, Fe(II) oxidation processes, for example, fast Fe^{2+} oxidation by O_2, are limiting Fe^{2+} availability.[14] However, considering Fe(III) photoreduction and Fe^{2+} mobilization from metastable FeS_x as important Fe^{2+} sources in marine sediments, the additionally produced Fe^{2+} is expected to be used as nutrient or as substrate by Fe(II)-oxidizing bacteria. The mineral transformations might also lead to desorption of adsorbed Fe(II) or other nutrients or pollutants (e.g., heavy metals)[20−23] and lead to regeneration of the sediment by providing fresh Fe mineral reaction sites. The high reactivity of metastable FeS_x might drive a fast turnover of Fe(II) in the sediment. Although the concentration profiles were recorded in single sediment cores, the starting conditions of all incubated sediment cores were the same due to homogenization of the sediment, and we therefore obtained consistent temporal and spatial data that show that the Fe^{2+} distribution in sediments is highly sensitive and dynamic and changes drastically toward less crystalline Fe solid phases and the release of high amounts of Fe^{2+} as a consequence of chemical changes caused by physical disturbances and/or the introduction of oxidants. The fast readjustment of O_2 gradients in the sediment[38,39] may give the impression that pre-storm redox conditions are quickly re-established after storm events. However, based on the interactions between dissolved and metastable Fe phases, we showed that the Fe geochemistry in sediments is highly variable with highly reactive intermediates playing a key role in sedimentary Fe cycling and bioavailability. This study demonstrated that the fast Fe^{2+} mobilization as a result of physical perturbation is an overlooked Fe(II) source, which likely makes an important contribution to Fe and other biogeochemical cycles in sediments.

■ ASSOCIATED CONTENT

Supporting Information

The Supporting Information is available free of charge at https://pubs.acs.org/doi/10.1021/acs.est.9b06278.

Images showing sediment cores that were prepared for incubation, scheme of the experimental approach, O_2 concentration profiles after 1, 2, and 7 days of undisturbed 12 h light−dark incubation and 1 day after the simulated storm event, light intensity (expressed as scalar irradiance) in the sediment, Fe^{2+} concentration profiles after 5, 6, and 7 days of undisturbed 12 h light−dark incubation, Fe^{2+} develop-

https://dx.doi.org/10.1021/acs.est.9b06278
Environ. Sci. Technol. 2020, 54, 3209−3218

ment during a simulated storm event in the sediment core determined by voltammetric measurements, impact of physical movement (slicing and homogenization) of sediment on Fe^{2+} mobilization, profiles in in situ sediment cores before and 2 days after a storm at the sampling field site, pH profile recorded before the 2nd simulated storm event, table listing Mössbauer spectroscopy parameters, representative Mössbauer model fit of spectra, and X-ray diffraction pattern collected from the native sample material and the dried sediment material (PDF)

AUTHOR INFORMATION

Corresponding Author

Caroline Schmidt − *Geomicrobiology Group, Center for Applied Geoscience (ZAG), University of Tuebingen, D-72076 Tuebingen, Germany;* orcid.org/0000-0001-8472-808X; Phone: +49-7071-2975496; Email: caroline.schmidt@uni-tuebingen.de; Fax: +49-7071-29-295059

Authors

Ulf Lueder − *Geomicrobiology Group, Center for Applied Geoscience (ZAG), University of Tuebingen, D-72076 Tuebingen, Germany*

Markus Maisch − *Geomicrobiology Group, Center for Applied Geoscience (ZAG), University of Tuebingen, D-72076 Tuebingen, Germany*

Katja Laufer − *Center for Geomicrobiology, Department of Bioscience, Aarhus University, 8000 Aarhus, Denmark; GEOMAR Helmholtz Center for Ocean Research Kiel, 24148 Kiel, Germany*

Bo Barker Jørgensen − *Center for Geomicrobiology, Department of Bioscience, Aarhus University, 8000 Aarhus, Denmark*

Andreas Kappler − *Geomicrobiology Group, Center for Applied Geoscience (ZAG), University of Tuebingen, D-72076 Tuebingen, Germany; Center for Geomicrobiology, Department of Bioscience, Aarhus University, 8000 Aarhus, Denmark;* orcid.org/0000-0002-3558-9500

Complete contact information is available at: https://pubs.acs.org/10.1021/acs.est.9b06278

Notes

The authors declare no competing financial interest.

ACKNOWLEDGMENTS

The authors acknowledge Alissa Findlay for her support during data discussion. C.S. received funding from a Margarete von Wrangell fellowship (Ministry of Baden-Württemberg, Germany) and the DFG grant (SCHM2808/4-1). K.L. was supported by a DFG research fellowship (DFG 389371177).

REFERENCES

(1) Kappler, A.; Straub, K. L. Geomicrobiological cycling of iron. *Rev. Mineral. Geochem.* **2005**, *59*, 85−108.

(2) Melton, E. D.; Swanner, E. D.; Behrens, S.; Schmidt, C.; Kappler, A. The interplay of microbially mediated and abiotic reactions in the biogeochemical Fe cycle. *Nat. Rev. Microbiol.* **2014**, *12*, 797−808.

(3) Laufer, K.; Nordhoff, M.; Røy, H.; Schmidt, C.; Behrens, S.; Jørgensen, B. B.; Kappler, A. Coexistence of microaerophilic, nitrate-reducing, and phototrophic Fe(II)-oxidizers and Fe(III)-reducers in coastal marine sediment. *Appl. Environ. Microbiol.* **2016**, *82*, 1433−1447.

(4) Otte, J. M.; Harter, J.; Laufer, K.; Blackwell, N.; Straub, D.; Kappler, A.; Kleindienst, S. The distribution of active iron-cycling bacteria in marine and freshwater sediments is decoupled from geochemical gradients. *Environ. Microbiol.* **2018**, *20*, 2483−2499.

(5) Laufer, K.; Nordhoff, M.; Halama, M.; Martinez, R. E.; Obst, M.; Nowak, M.; Stryhanyuk, H.; Richnow, H. H.; Kappler, A. Microaerophilic Fe(II)-oxidizing Zetaproteobacteria isolated from low-Fe marine coastal sediments: physiology and composition of their twisted stalks. *Appl. Environ. Microbiol.* **2017**, *83*, e03118−e03116.

(6) McAllister, S. M.; Moore, R. M.; Gartman, A.; Luther, G. W., III; Emerson, D.; Chan, C. S. The Fe(II)-oxidizing Zetaproteobacteria: historical, ecological and genomic perspectives. *FEMS Microbiol. Ecol.* **2019**, *95*, fiz015.

(7) Lueder, U.; Jørgensen, B. B.; Kappler, A.; Schmidt, C. Fe(III) Photoreduction Producing Feaq2+in Oxic Freshwater Sediment. *Environ. Sci. Technol.* **2019**, *54*, 862−869.

(8) Lovley, D. R.; Phillips, E. J. P. Novel mode of microbial energy metabolism: organic carbon oxidation coupled to dissimilatory reduction of iron or manganese. *Appl. Environ. Microbiol.* **1988**, *54*, 1472−1480.

(9) Lovley, D. R. Dissimilatory Fe(III) and Mn(IV) reduction. *Microbiol. Rev.* **1991**, *55*, 259−287.

(10) Kashefi, K.; Tor, J. M.; Holmes, D. E.; Gaw Van Praagh, C. V.; Reysenbach, A.-L.; Lovley, D. R. Geoglobus ahangari gen. nov., sp. nov., a novel hyperthermophilic archaeon capable of oxidizing organic acids and growing autotrophically on hydrogen with Fe(III) serving as the sole electron acceptor. *Int. J. Syst. Evol. Microbiol.* **2002**, *52*, 719−728.

(11) Pyzik, A. J.; Sommer, S. E. Sedimentary iron monosulfides: Kinetics and mechanism of formation. *Geochim. Cosmochim. Acta* **1981**, *45*, 687−698.

(12) Canfield, D. E. Reactive iron in marine sediments. *Geochim. Cosmochim. Acta* **1989**, *53*, 619−632.

(13) Sulzberger, B.; Suter, D.; Siffert, C.; Banwart, S.; Stumm, W. Dissolution of Fe(III)(hydr)oxides in natural waters; laboratory assessment on the kinetics controlled by surface coordination. *Mar. Chem.* **1989**, *28*, 127−144.

(14) Millero, F. J.; Sotolongo, S.; Izaguirre, M. The oxidation kinetics of Fe(II) in seawater. *Geochim. Cosmochim. Acta* **1987**, *51*, 793−801.

(15) Burdige, D. J. The biogeochemistry of manganese and iron reduction in marine sediments. *Earth-Sci. Rev.* **1993**, *35*, 249−284.

(16) Davison, W.; Grime, G. W.; Morgan, J. A. W.; Clarke, K. Distribution of dissolved iron in sediment pore waters at submillimetre resolution. *Nature* **1991**, *352*, 323−325.

(17) Schmidt, C.; Behrens, S.; Kappler, A. Ecosystem functioning from a geomicrobiological perspective a conceptual framework for biogeochemical iron cycling. *Environ. Chem.* **2010**, *7*, 399−405.

(18) Canfield, D. E.; Thamdrup, B.; Hansen, J. W. The anaerobic degradation of organic matter in Danish coastal sediments: Iron reduction, manganese reduction, and sulfate reduction. *Geochim. Cosmochim. Acta* **1993**, *57*, 3867−3883.

(19) Haese, R. R.; Petermann, H.; Dittert, L.; Schulz, H. D. The early diagenesis of iron in pelagic sediments: a multidisciplinary approach. *Earth Planet. Sci. Lett.* **1998**, *157*, 233−248.

(20) Dixit, S.; Hering, J. G. Comparison of arsenic(V) and arsenic(III) sorption onto iron oxide minerals: Implications for arsenic mobility. *Environ. Sci. Technol.* **2003**, *37*, 4182−4189.

(21) Giammar, D. E.; Hering, J. G. Time scales for sorption−desorption and surface precipitation of uranyl on goethite. *Environ. Sci. Technol.* **2001**, *35*, 3332−3337.

(22) Su, C.; Suarez, D. L. Selenate and selenite sorption on iron oxides An infrared and electrophoretic study 1. *Soil Sci. Soc. Am. J.* **2000**, *64*, 101−111.

(23) Khare, N.; Hesterberg, D.; Martin, J. D. XANES investigation of phosphate sorption in single and binary systems of iron and aluminum oxide minerals. *Environ. Sci. Technol.* **2005**, *39*, 2152−2160.

(24) Berner, R. A. Sedimentary pyrite formation: An update. *Geochim. Cosmochim. Acta* **1984**, *48*, 605−615.

(25) Canfield, D. E.; Raiswell, R.; Bottrell, S. H. The reactivity of sedimentary iron minerals toward sulfide. *Am. J. Sci.* **1992**, *292*, 659−683.
(26) Rickard, D. Experimental concentration-time curves for the iron(II) sulphide precipitation process in aqueous solutions and their interpretation. *Chem. Geol.* **1989**, *78*, 315−324.
(27) Jørgensen, B. B. Mineralization of organic matter in the sea bed—the role of sulphate reduction. *Nature* **1982**, *296*, 643−645.
(28) Jørgensen, B. B. The sulfur cycle of a coastal marine sediment (Limfjorden, Denmark)[1]. *Limnol. Oceanogr.* **1977**, *22*, 814−832.
(29) Luther, G. W., III; Giblin, A.; Howarth, R. W.; Ryans, R. A. Pyrite and oxidized iron mineral phases formed from pyrite oxidation in salt marsh and estuarine sediments. *Geochim. Cosmochim. Acta* **1982**, *46*, 2665−2669.
(30) Boesen, C.; Postma, D. Pyrite formation in anoxic environments of the Baltic. *Am. J. Sci.* **1988**, *288*, 575−603.
(31) Howarth, R. W. Pyrite: Its rapid formation in a salt marsh and its importance in ecosystem metabolism. *Science* **1979**, *203*, 49−51.
(32) Aller, R. C.; Charnock, H.; Edmond, J. M.; McCave, I. N.; Rice, A. L.; Wilson, T. R. S. Bioturbation and manganese cycling in hemipelagic sediments. *Philos. Trans. R. Soc. London. Ser. A* **1990**, *331*, 51−68.
(33) Thamdrup, B.; Fossing, H.; Jørgensen, B. B. Manganese, iron and sulfur cycling in a coastal marine sediment, Aarhus bay, Denmark. *Geochim. Cosmochim. Acta* **1994**, *58*, 5115−5129.
(34) Brand, A.; Lacy, J. R.; Hsu, K.; Hoover, D.; Gladding, S.; Stacey, M. T. Wind-enhanced resuspension in the shallow waters of South San Francisco Bay: Mechanisms and potential implications for cohesive sediment transport. *J. Geophys. Res.: Oceans* **2010**, *115*, C11024.
(35) You, Z.-J. Fine sediment resuspension dynamics in a large semi-enclosed bay. *Ocean Eng.* **2005**, *32*, 1982−1993.
(36) Ward, L. G.; Michael Kemp, W.; Boynton, W. R. The influence of waves and seagrass communities on suspended particulates in an estuarine embayment. *Mar. Geol.* **1984**, *59*, 85−103.
(37) Sanford, L. P. Wave-forced resuspension of upper Chesapeake Bay muds. *Estuaries* **1994**, *17*, 148−165.
(38) Epping, E.; Kühl, M. The responses of photosynthesis and oxygen consumption to short-term changes in temperature and irradiance in a cyanobacterial mat (Ebro Delta, Spain). *Environ. Microbiol.* **2000**, *2*, 465−474.
(39) Gerhardt, S.; Brune, A.; Schink, B. Dynamics of redox changes of iron caused by light−dark variations in littoral sediment of a freshwater lake. *Biogeochemistry* **2005**, *74*, 323−339.
(40) Brendel, P. J.; Luther, G. W., III Development of a gold amalgam voltammetric microelectrode for the determination of dissolved Fe, Mn, O2, and S(-II) in porewaters of marine and freshwater sediments. *Environ. Sci. Technol.* **1995**, *29*, 751−761.
(41) Slowey, A. J.; Marvin-DiPasquale, M. How to overcome inter-electrode variability and instability to quantify dissolved oxygen, Fe(II), Mn(II), and S(II) in undisturbed soils and sediments using voltammetry. *Geochem. Trans.* **2012**, *13*, 6.
(42) Bristow, G.; Taillefert, M. VOLTINT: A Matlab®-based program for semi-automated processing of geochemical data acquired by voltammetry. *Comput. Geosci.* **2008**, *34*, 153−162.
(43) Revsbech, N. P. An oxygen microsensor with a guard cathode. *Limnol. Oceanogr.* **1989**, *34*, 474−478.
(44) Kühl, M.; Jørgensen, B. B. Spectral light measurements in microbenthic phototrophic communities with a fiber-optic microprobe coupled to a sensitive diode array detector. *Limnol. Oceanogr.* **1992**, *37*, 1813−1823.
(45) Roden, E. E.; Zachara, J. M. Microbial reduction of crystalline iron(III) oxides: Influence of oxide surface area and potential for cell growth. *Environ. Sci. Technol.* **1996**, *30*, 1618−1628.
(46) Tessier, A.; Campbell, P. G. C.; Bisson, M. Sequential extraction procedure for the speciation of particulate trace metals. *Anal. Chem.* **1979**, *51*, 844−851.
(47) Shannon, R. D.; White, J. R. The selectivity of a sequential extraction procedure for the determination of iron oxyhydroxides andiron sulfides in lake sediments. *Biogeochemistry* **1991**, *14*, 193−208.
(48) Heron, G.; Crouzet, C.; Bourg, A. C. M.; Christensen, T. H. Speciation of Fe(II) and Fe(III) in contaminated aquifer sediments using chemical extraction techniques. *Environ. Sci. Technol.* **1994**, *28*, 1698−1705.
(49) Stookey, L. L. Ferrozine - a new spectrophotometric reagent for iron. *Anal. Chem.* **1970**, *42*, 779−781.
(50) Rancourt, D. G.; Ping, J. Y. Voigt-based methods for arbitrary-shape static hyperfine parameter distributions in Mössbauer spectroscopy. *Nucl. Instrum. Methods Phys. Res., Sect. B* **1991**, *58*, 85−97.
(51) Jørgensen, B. B.; Revsbech, N. P.; Blackburn, T. H.; Cohen, Y. Diurnal cycle of oxygen and sulfide microgradients and microbial photosynthesis in a cyanobacterial mat sediment. *Appl. Environ. Microbiol.* **1979**, *38*, 46−58.
(52) Lassen, C.; Ploug, H.; Jorgensen, B. B. Microalgal photosynthesis and spectral scalar irradiance in coastal marine sediments of Limfjorden, Denmark. *Limnol. Oceanogr.* **1992**, *37*, 760−772.
(53) Peng, C.; Bryce, C.; Sundman, A.; Kappler, A. Cryptic cycling of complexes containing Fe(III) and organic matter by phototrophic Fe(II)-oxidizing bacteria. *Appl. Environ. Microbiol.* **2019**, *85*, No. e02826.
(54) Taillefert, M.; Bono, A. B.; Luther, G. W., III Reactivity of freshly formed Fe(III) in synthetic solutions and (pore)waters: voltammetric evidence of an aging process. *Environ. Sci. Technol.* **2000**, *34*, 2169−2177.
(55) Laufer, K.; Byrne, J. M.; Glombitza, C.; Schmidt, C.; Jørgensen, B. B.; Kappler, A. Anaerobic microbial Fe(II) oxidation and Fe(III) reduction in coastal marine sediments controlled by organic carbon content. *Environ. Microbiol.* **2016**, *18*, 3159−3174.
(56) Boyd, P. W.; Watson, A. J.; Law, C. S.; Abraham, E. R.; Trull, T.; Murdoch, R.; Bakker, D. C. E.; Bowie, A. R.; Buesseler, K. O.; Chang, H.; Charette, M.; Croot, P.; Downing, K.; Frew, R.; Gall, M.; Hadfield, M.; Hall, J.; Harvey, M.; Jameson, G.; LaRoche, J.; Liddicoat, M.; Ling, R.; Maldonado, M. T.; McKay, R. M.; Nodder, S.; Pickmere, S.; Pridmore, R.; Rintoul, S.; Safi, K.; Sutton, P.; Strzepek, R.; Tanneberger, K.; Turner, S.; Waite, A.; Zeldis, J. A mesoscale phytoplankton bloom in the polar Southern Ocean stimulated by iron fertilization. *Nature* **2000**, *407*, 695−702.
(57) Boyd, P. W.; Ellwood, M. J. The biogeochemical cycle of iron in the ocean. *Nat. Geosci.* **2010**, *3*, 675.
(58) King, A. L.; Barbeau, K. A. Dissolved iron and macronutrient distributions in the southern California Current System. *J. Geophys. Res.: Oceans* **2011**, *116*, C03018.
(59) Elrod, V. A.; Berelson, W. M.; Coale, K. H.; Johnson, K. S. The flux of iron from continental shelf sediments: A missing source for global budgets. *Geophys. Res. Lett.* **2004**, *31*, L12307.
(60) Kuma, K.; Nakabayashi, S.; Suzuki, Y.; Kudo, I.; Matsunaga, K. Photo-reduction of Fe(III) by dissolved organic substances and existence of Fe(II) in seawater during spring blooms. *Mar. Chem.* **1992**, *37*, 15−27.
(61) O'Sullivan, D. W.; Hanson, A. K.; Miller, W. L.; Kester, D. R. Measurement of Fe(II) in surface water of the equatorial Pacific. *Limnol. Oceanogr.* **1991**, *36*, 1727−1741.
(62) Krachler, R.; Krachler, R. F.; von der Kammer, F.; Süphandag, A.; Jirsa, F.; Ayromlou, S.; Hofmann, T.; Keppler, B. K. Relevance of peat-draining rivers for the riverine input of dissolved iron into the ocean. *Sci. Total Environ.* **2010**, *408*, 2402−2408.
(63) Aller, R. C. Bioturbation and remineralization of sedimentary organic matter: effects of redox oscillation. *Chem. Geol.* **1994**, *114*, 331−345.
(64) Hines, M. E.; Orem, W. H.; Lyons, W. B.; Jones, G. E. Microbial activity and bioturbation-induced oscillations in pore water chemistry of estuarine sediments in spring. *Nature* **1982**, *299*, 433−435.
(65) Jing, L.; Ridd, P. V. Wave-current bottom shear stresses and sediment resuspension in Cleveland Bay, Australia. *Coastal Eng.* **1996**, *29*, 169−186.

https://dx.doi.org/10.1021/acs.est.9b06278
Environ. Sci. Technol. 2020, 54, 3209−3218

(66) Scheffer, M.; Portielje, R.; Zambrano, L. Fish facilitate wave resuspension of sediment. *Limnol. Oceanogr.* **2003**, *48*, 1920−1926.
(67) Colijn, F.; van Buurt, G. Influence of light and temperature on the photosynthetic rate of marine benthic diatoms. *Mar. Biol.* **1975**, *31*, 209−214.
(68) Whitney, D. E.; Darley, W. M. Effect of light intensity upon salt marsh benthic microalgal photosynthesis. *Mar. Biol.* **1983**, *75*, 249−252.
(69) MacIntyre, H. L.; Geider, R. J.; Miller, D. C. Microphytobenthos: The ecological role of the "secret garden" of unvegetated, shallow-water marine habitats. I. Distribution, abundance and primary production. *Estuaries* **1996**, *19*, 186−201.
(70) Aller, R. C. Diagenetic processes near the sediment-water interface of Long Island Sound. II. Fe and Mn. In *Advances in Geophysics;* Saltzman, B., Ed. Elsevier: 1980; Vol. *22*, pp 351−415.
(71) Thiel, J.; Byrne, J.; Kappler, A.; Schink, B.; Pester, M. Pyrite formation from FeS and H_2S is mediated by a novel type of microbial energy metabolism. *bioRxiv* **2018**, 396978.
(72) Rickard, D.; Oldroyd, A.; Cramp, A. Voltammetric evidence for soluble FeS complexes in anoxic estuarine muds. *Estuaries* **1999**, *22*, 693−701.
(73) Davison, W.; Buffle, J.; DeVitre, R. Voltammetric characterization of a dissolved iron sulphide species by laboratory and field studies. *Anal. Chim. Acta* **1998**, *377*, 193−203.
(74) Theberge, S. M.; Luther, G. W., III Determination of the electrochemical properties of a soluble aqueous FeS species present in sulfidic solutions. *Aquat. Geochem.* **1997**, *3*, 191−211.
(75) Luther, G. W.; Rickard, D. T.; Theberge, S.; Olroyd, A. Determination of metal (bi)sulfide stability constants of Mn2+, Fe2+, Co2+, Ni2+, Cu2+, and Zn2+ by voltammetric methods. *Environ. Sci. Technol.* **1996**, *30*, 671−679.
(76) Cornwell, J. C.; Morse, J. W. The characterization of iron sulfide minerals in anoxic marine sediments. *Mar. Chem.* **1987**, *22*, 193−206.
(77) Howarth, R. W.; Jørgensen, B. B. Formation of ^{35}S-labelled elemental sulfur and pyrite in coastal marine sediments (Limfjorden and Kysing Fjord, Denmark) during short-term $^{35}SO_4^{2-}$ reduction measurements. *Geochim. Cosmochim. Acta* **1984**, *48*, 1807−1818.
(78) Moses, C. O.; Kirk Nordstrom, D.; Herman, J. S.; Mills, A. L. Aqueous pyrite oxidation by dissolved oxygen and by ferric iron. *Geochim. Cosmochim. Acta* **1987**, *51*, 1561−1571.
(79) Moses, C. O.; Herman, J. S. Pyrite oxidation at circumneutral pH. *Geochim. Cosmochim. Acta* **1991**, *55*, 471−482.
(80) Schippers, A.; Jørgensen, B. B. Biogeochemistry of pyrite and iron sulfide oxidation in marine sediments. *Geochim. Cosmochim. Acta* **2002**, *66*, 85−92.
(81) Poulton, S. W.; Canfield, D. E. Development of a sequential extraction procedure for iron: implications for iron partitioning in continentally derived particulates. *Chem. Geol.* **2005**, *214*, 209−221.
(82) Morse, J. W.; Casey, W. H. Ostwald processes and mineral paragenesis in sediments. *Am. J. Sci.* **1988**, *288*, 537−560.
(83) Roden, E. E. Fe(III) oxide reactivity toward biological versus chemical reduction. *Environ. Sci. Technol.* **2003**, *37*, 1319−1324.
(84) Postma, D. The reactivity of iron oxides in sediments: A kinetic approach. *Geochim. Cosmochim. Acta* **1993**, *57*, 5027−5034.
(85) Hansel, C. M.; Benner, S. G.; Nico, P.; Fendorf, S. Structural constraints of ferric (hydr)oxides on dissimilatory iron reduction and the fate of Fe(II). *Geochim. Cosmochim. Acta* **2004**, *68*, 3217−3229.
(86) Cutting, R. S.; Coker, V. S.; Fellowes, J. W.; Lloyd, J. R.; Vaughan, D. J. Mineralogical and morphological constraints on the reduction of Fe(III) minerals by Geobacter sulfurreducens. *Geochim. Cosmochim. Acta* **2009**, *73*, 4004−4022.
(87) Wan, M.; Schröder, C.; Peiffer, S. Fe(III):S(-II) concentration ratio controls the pathway and the kinetics of pyrite formation during sulfidation of ferric hydroxides. *Geochim. Cosmochim. Acta* **2017**, *217*, 334−348.
(88) Schoonen, M. A. A.; Barnes, H. L. Reactions forming pyrite and marcasite from solution: II. Via FeS precursors below 100°C. *Geochim. Cosmochim. Acta* **1991**, *55*, 1505−1514.
(89) Giblin, A. E.; Howarth, R. W. Porewater evidence for a dynamic sedimentary iron cycle in salt marshes1. *Limnol. Oceanogr.* **1984**, *29*, 47−63.

https://dx.doi.org/10.1021/acs.est.9b06278
Environ. Sci. Technol. 2020, 54, 3209−3218